

# Uplink Capacity of A Cellular System Using Multi-user Single-carrier MIMO Multiplexing Combined with Frequency-domain Equalization and Transmit Power Control

Takahiro Chiba · Kazuaki Takeda · Kazuki Takeda · Fumiyuki Adachi

© Springer Science+Business Media, LLC. 2010

**Abstract** Multi-user single-carrier multiple-input multiple-output (MU SC-MIMO) multiplexing can increase the uplink capacity of a cellular system without expanding the signal bandwidth. It is practically important to make clear an extent to which the MU SC-MIMO multiplexing combined with frequency-domain equalization (FDE) and transmit power control (TPC) can increase the uplink capacity in the presence of the co-channel interference (CCI). Since the theoretical analysis is quite difficult, we resort to the computer simulation to investigate the uplink capacity. In this paper, frequency-domain zero-forcing detection (ZFD) and frequency-domain minimum mean square error detection (MMSED) are considered for MU signal detection. It is shown that ZFD and MMSED provide almost the same uplink capacity and that an advantage of fast TPC over slow TPC diminishes. As a result, MU SC-MIMO using computationally efficient ZFD can be used together with slow TPC instead of using MMSED. With 8 receive antennas and slow TPC, MU SC-MIMO multiplexing using ZFD can achieve about 1.5 times higher uplink capacity than SU SC-SIMO diversity.

**Keywords** Multi-user MIMO · Single-carrier · Frequency-domain equalization · Cellular system · Uplink-capacity

## 1 Introduction

Broadband data services are demanded in next-generation mobile communication systems [1]. Broadband wireless channel consists of many propagation paths having different time delays, resulting in frequency-selective fading [2]. Recently, broadband single-carrier (SC) transmission has been attracting a lot of attention because of its low peak-to-average power ratio (PAPR) property and because the frequency diversity gain can be obtained by the use of frequency-domain equalization (FDE) [3,4]. In cellular systems, the same carrier frequency

---

T. Chiba · K. Takeda · K. Takeda · F. Adachi (✉)  
Department of Electrical and Communication Engineering, Graduate School of Engineering,  
Tohoku University, 6-6-05 Aza-Aoba, Aramaki, Aoba-ku, Sendai-shi 980-8579, Japan  
e-mail: adachi@ecei.tohoku.ac.jp

is reused in spatially separated different cells to efficiently utilize the limited bandwidth [5]. However, only reusing the same carrier frequency is not sufficient for offering broadband services in cellular systems with the limited bandwidth.

To increase the uplink capacity with the limited bandwidth, multi-user multiple-input multiple-output (MU MIMO) multiplexing [6–9] can be used. MU SC-MIMO multiplexing is promising for the uplink applications owing to its low PAPR property [10,11]. Several signal detection schemes exist combined with FDE for MU SC-MIMO multiplexing, e.g., frequency-domain zero-forcing detection (ZFD) [12] and frequency-domain minimum mean square error detection (MMSED) [13]. In a cellular system, a user who is located close to the cell edge suffers from large power loss due to shadowing loss and path loss as well as fading [14]. To eliminate the power loss problem, transmit power control (TPC) can be used [15]; however, in return, this increases the co-channel interference (CCI) to other cells.

Many studies on the information theoretic capacity and the sum capacity achievable by MU SC-MIMO multiplexing in a cellular system can be found in the literature, e.g., [16–19]. However, to the best of authors' knowledge, it is not clear to which extent the MU SC-MIMO multiplexing combined with FDE and TPC can increase the uplink capacity in a cellular system.

In this paper, since the theoretical analysis is quite difficult, we investigate by the computer simulation the uplink capacity of a broadband cellular system using MU SC-MIMO multiplexing combined with FDE and TPC. The remainder of this paper is organized as follows. Section 2 presents the MU SC-MIMO cellular system model. MU SC-MIMO multiplexing combined with FDE and TPC is described in Sect. 3. Frequency-domain ZFD and frequency-domain MMSED are considered as the signal detection. In Sect. 4, the uplink capacity of MU SC-MIMO multiplexing is discussed. Section 5 concludes this paper.

## 2 MU SC-MIMO Cellular System Model

In a cellular system, the available channels are divided into a number of channel groups and each channel group is reused in different cells [5]. The number  $N$  of different channel groups is called the cluster size. The smaller the cluster size becomes, the more channels can be assigned to each cell. In this paper, it is assumed that  $U$  users in each cell are simultaneously transmitting their data by using the same carrier frequency. Figure 1 illustrates the uplink CCI model for MU SC-MIMO multiplexing. In this paper, only 6 nearest co-channel cells ( $c = 1 \sim 6$ ) surrounding the desired cell ( $c = 0$ ) are considered since they are the predominant cause of CCI which degrades the uplink capacity. The CCI power becomes weaker by

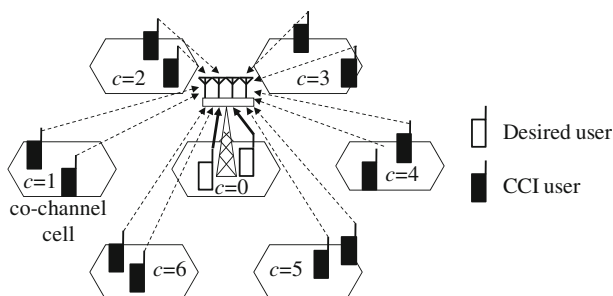


**Fig. 1** CCI model

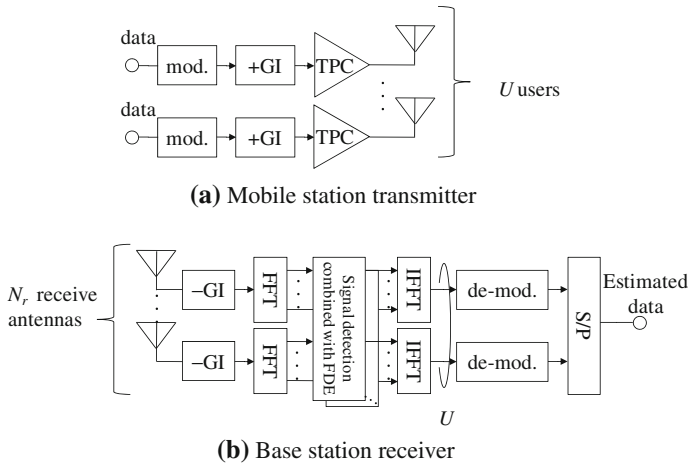
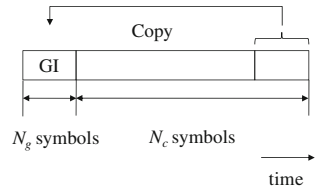


Fig. 2 Uplink transmission system model

Fig. 3 Transmit symbol block



increasing the distance between the co-channel cells or the cluster size  $N$ ; however, in return, this reduces the number of channels in one channel group which can be assigned to each cell, resulting in the reduced uplink capacity.

In this paper, the normalized transmit power and distance are introduced. By denoting the transmit power by  $P$ , the received signal power  $P(r)$  (assuming no shadowing loss and fading) for a user who is located at the distance  $r$  from its communicating base station (BS) is given by  $P(r) = P \times r^{-\alpha} = (P \cdot R^{-\alpha}) \times (r/R)^{-\alpha}$ , where  $\alpha$  is the distance-dependent path loss exponent and  $R$  is the cell radius. When the TPC with its target  $P_{\text{tpc}}$  is used and ignoring the shadowing loss and fading, the transmit signal power is given by  $P(r) = P_{\text{tpc}} \times r^\alpha = (P_{\text{tpc}} \cdot R^\alpha) \times (r/R)^\alpha$ . For the simplicity purpose in this paper,  $P \cdot R^{-\alpha}$ ,  $P_{\text{tpc}} \cdot R^\alpha$ , and  $r/R$  are simply represented by  $P$ ,  $P_{\text{tpc}}$ , and  $r$  ( $0 < r \leq 1$ ), respectively.  $P$ ,  $P_{\text{tpc}}$ , and  $r$  are called the normalized transmit power, the normalized TPC target, and the normalized distance, respectively.

The uplink transmission in the desired cell ( $c = 0$ ) is considered. Figure 2 illustrates the uplink transmission system model of MU SC-MIMO multiplexing with FDE. It is assumed that each user has the single transmit antenna and a base station (BS) of each cell has  $N_r$  ( $\geq U$ ) receive antennas. At a mobile transmitter, each user’s binary data sequence is data-modulated and divided into a sequence of blocks of  $N_c$  symbols each. The last  $N_g$  symbols in each block are copied and inserted as a cyclic prefix into the guard interval (GI), placed at the beginning of each block, to form a block of  $N_g + N_c$  symbols (see Fig. 3) [3].

The transmit timing offset plus maximum propagation time delay among  $U$  users of the  $c = 0$ -th cell is assumed to be less than the GI length. It should be noted that the CCIs from 6 co-channel cells ( $c = 1 \sim 6$ ) are time-asynchronous to the signals of the desired  $c = 0$ -th cell. At the BS receiver of the  $c = 0$ -th cell, a superposition of  $U$  users’ transmitted signals

corrupted by the CCI is received by  $N_r$  receive antennas. After the removal of the GI from the received signal,  $N_c$ -point fast Fourier transform (FFT) is applied to transform the GI-removed received signal into the frequency-domain signal. After performing signal detection combined with FDE, each user's frequency-domain signals are transformed back into time-domain signal block by using  $N_c$ -point inverse FFT (IFFT) and then, data demodulation is done.

### 3 Signal Detection Combined with FDE and TPC

The uplink capacity depends on the propagation environment. There have been many works on the realistic propagation modeling of MIMO systems [20,21]. However, the realistic propagation model is too complex to draw a general conclusion. In this paper, we use the following simple and popular channel model [16,17,22,23]:

- (a) Assuming non line of sight (NLoS) channel between each user and BS, the channel is characterized by the distance-dependent path-loss, fading loss, and frequency-selective Rayleigh fading.
- (b) The shadowing loss associated with a different user is uncorrelated. The frequency-selective Rayleigh fading associated with a different user is also uncorrelated.
- (c) Assuming broadband transmissions, the variations in the path-loss, shadowing loss and fading stay constant during the transmission of one signal block of  $N_g + N_c$  symbols, but, fading changes block by block due to the user mobility.

Without loss of generality, a transmission of one block of  $N_c$  symbols from each user is considered. Throughout the paper, symbol-spaced discrete-time signal representation is used. First, we give the received signal representation and then, the MU SC-MIMO signal detection combined with FDE and TPC is presented. In the following, for the sake of simplicity, we omit the insertion and removal of the GI.

#### 3.1 Received Signal

The  $t$ -th ( $t = 0 \sim N_c - 1$ ) transmit signal from  $u$ -th user in the  $c$ -th cell is denoted by  $\sqrt{2P_{0(c)}}s_{0(c)}(t)$ , where  $s_{u(c)}(t)$  and  $P_{u(c)}$  are the data-modulated symbol and the transmit power, respectively. The transmit signals from  $U$  users are represented using the vector form as  $\mathbf{s}_c(t) = [\sqrt{2P_{0(c)}}s_{0(c)}(t), \sqrt{2P_{1(c)}}s_{1(c)}(t), \dots, \sqrt{2P_{u(c)}}s_{u(c)}(t), \dots, \sqrt{2P_{U-1(c)}}s_{U-1(c)}(t)]^T$ , where  $(\cdot)^T$  denotes the transposition. Each user's transmitted signal passes through a different frequency-selective fading channel. The channel impulse response between the  $u$ -th user in the  $c$ -th cell and the  $m$ -th receive antenna of the BS of the  $c = 0$ -th cell is given by

$$\tilde{h}_{m(0),u(c)}(t) = \sqrt{r_{0,u(c)}^{-\alpha} \cdot 10^{-\frac{\eta_{0,u(c)}}{10}}} \sum_{l=0}^{L-1} h_{m(0),u(c)}^{(l)} \cdot \delta(t - \tau_{u(c),l}), \quad (1)$$

where  $r_{0,u(c)}$ ,  $\eta_{0,u(c)}$ , and  $\alpha$  denote the normalized distance between the  $u$ -th user in the  $c$ -th cell and the BS of the  $c = 0$ -th cell, the shadowing loss in dB, and the path loss exponent, respectively. In Eq. (1), the variable  $l (= 0 \sim L - 1)$  represents the path index and  $h_{m(0),u(c)}^{(l)}$  and  $\tau_{u(c),l}$  are respectively the complex-valued path gain with  $\sum_{l=0}^{L-1} E \left[ |h_{m(0),u(c)}^{(l)}|^2 \right] = 1$  ( $E[\cdot]$  denotes the ensemble average operation) and the time delay between the  $u$ -th user in

the  $c$ -th cell and the BS of the  $c = 0$ -th cell. Using the matrix representation, the received signal vector of the  $c = 0$ -th cell can be expressed as

$$\mathbf{y}(t) = [y_{0(0)}(t), \dots, y_{m(0)}(t), \dots, y_{N_r-1(0)}(t)]^T$$

$$= \sum_{l=0}^{L-1} \tilde{\mathbf{h}}_0^{(l)} \cdot \mathbf{s}_0((t - \tau_{u(0),l}) \bmod N_c) + \sum_{c=1}^6 \sum_{l=0}^{L-1} \tilde{\mathbf{h}}_c^{(l)} \cdot \mathbf{i}_c(t - \tau_{u(c),l}) + \mathbf{n}(t), \quad (2)$$

where  $y_{m(0)}(t)$ ,  $m = 0 \sim N_r - 1$ ,  $t = 0 \sim N_c - 1$ , represents the  $t$ -th received signal of the  $m$ -th receive antenna at the BS of the  $c = 0$ -th cell and the first and second terms are the desired signal and the CCI, respectively.  $\tilde{\mathbf{h}}_c^{(l)}$  is the path gain matrix of size  $N_r \times U$  of the  $l$ -th path, the  $(m(0), u(c))$ -th element of which is given by  $\tilde{h}_{m(0),u(c)}^{(l)} = \sqrt{r_{u(c)}^{-\alpha}} \cdot 10^{-\frac{\eta_{0,u(c)}}{10}} h_{m(0),u(c)}^{(l)}$ .  $\mathbf{i}_c(t) = [\sqrt{2P_{0(c)}}i_{0(c)}(t), \dots, \sqrt{2P_{u(c)}}i_{u(c)}(t), \dots, \sqrt{2P_{U-1(c)}}i_{U-1(c)}(t)]^T$  is the CCI vector of size  $U \times 1$ , which represents the CCI from  $U$  users in the  $c$ -th cell, and  $\mathbf{n}(t) = [n_{0(0)}(t), \dots, n_{m(0)}(t), \dots, n_{N_r-1(0)}(t)]^T$  is the noise vector of size  $N_r \times 1$ , where  $\{n_{m(0)}(t); m(0) = 0 \sim N_r - 1\}$  are the independent zero-mean complex Gaussian variables with variance  $2\sigma_n^2$  due to additive white Gaussian noise (AWGN).

The received signal vector  $\mathbf{y}_0(t)$  is transformed into the frequency-domain signal vector  $\mathbf{Y}_0(k)$  by using an  $N_c$ -point FFT.  $\mathbf{Y}_0(k)$  can be expressed as

$$\mathbf{Y}_0(k) = \sum_{t=0}^{N_c-1} \mathbf{y}_0(t) \exp\left(-j2\pi k \frac{t}{N_c}\right) = \tilde{\mathbf{H}}_0(k)\mathbf{S}_0(k) + \mathbf{I}_0(k) + \mathbf{\Pi}_0(k), \quad (3)$$

where  $\tilde{\mathbf{H}}_c(k) = [\tilde{\mathbf{H}}_{0(c)}(k), \dots, \tilde{\mathbf{H}}_{u(c)}(k), \dots, \tilde{\mathbf{H}}_{U-1(c)}(k)]$  with  $\tilde{\mathbf{H}}_{u(c)}(k) = [\tilde{H}_{0(0),u(c)}(k), \dots, \tilde{H}_{m(0),u(c)}(k), \dots, \tilde{H}_{N_r-1(0),u(c)}(k)]^T$ ,  $\mathbf{S}_0(k) = [S_{0(0)}(k), \dots, S_{u(0)}(k), \dots, S_{U-1(0)}(k)]^T$ ,  $\mathbf{I}_0(k) = [I_{0(0)}(k), \dots, I_{m(0)}(k), \dots, I_{N_r-1(0)}(k)]^T$ , and  $\mathbf{\Pi}_0(k) = [\Pi_{0(0)}(k), \dots, \Pi_{m(0)}(k), \dots, \Pi_{N_r-1(0)}(k)]^T$  denote the channel gain matrix of size  $N_r \times U$ , the frequency-domain signal vector of size  $U \times 1$ , the CCI vector of size  $N_r \times 1$ , and the noise vector of size  $N_r \times 1$ , respectively. The  $m(0)$ -th element  $\tilde{H}_{m(0),u(c)}(k)$  of  $\tilde{\mathbf{H}}_{u(c)}(k)$  is given by

$$\tilde{H}_{m(0),u(c)}(k) = \sum_{l=0}^{L-1} \tilde{h}_{m(0),u(c)}^{(l)} \exp\left(-j2\pi k \frac{\tau_{u(c),l}}{N_c}\right) = \sqrt{r_{u(c)}^{-\alpha}} \cdot 10^{-\frac{\eta_{0,u(c)}}{10}} \cdot H_{m(0),u(c)}(k), \quad (4)$$

where  $H_{m(0),u(c)}(k)$  denotes the channel gain between the  $u$ -th user in the  $c$ -th cell and the  $m$ -th receive antenna of the  $c = 0$ -th cell BS.  $S_{u(0)}(k)$ ,  $I_{m(0)}(k)$ , and  $\Pi_{m(0)}(k)$  are given as

$$\begin{cases} S_{u(0)}(k) = \sqrt{2P_{u(0)}} \sum_{t=0}^{N_c-1} s_{u(0)}(t) \exp\left(-j2\pi k \frac{t}{N_c}\right) \\ I_{m(0)}(k) = \sum_{c=1}^6 \sqrt{2P_{u(c)}} \sum_{t=0}^{N_c-1} \sum_{u(c)=0}^{U-1} \sum_{l=0}^{L-1} \tilde{h}_{m(0),u(c)}^{(l)} \cdot i_{u(c)}(t - \tau_{u(c),l}) \exp\left(-j2\pi k \frac{t}{N_c}\right) \\ \Pi_{m(0)}(k) = \sum_{t=0}^{N_c-1} n_{m(0)}(t) \exp\left(-j2\pi k \frac{t}{N_c}\right) \end{cases} \quad (5)$$

### 3.2 Signal Detection

ZFD and MMSED [12, 13] are modified to be used for the MU SC-MIMO signal detection in the frequency-domain. The detector output vector is expressed using the matrix form as

$$\tilde{\mathbf{S}}_0(k) = \left[ \tilde{S}_{0(0)}(k), \dots, \tilde{S}_{u(0)}(k), \dots, \tilde{S}_{U-1(0)}(k) \right]^T = \mathbf{W}_0(k)\mathbf{Y}_0(k) \text{ for } k = 0 \sim N_c - 1, \tag{6}$$

where  $\mathbf{W}_0(k) = [\mathbf{w}_{0(0)}(k), \dots, \mathbf{w}_{m(0)}(k), \dots, \mathbf{w}_{N_r-1(0)}(k)]$  represents the weight matrix of size  $U \times N_r$  for the signal detection combined with FDE. ZFD perfectly restores the frequency-nonselective channel if the perfect knowledge of channel state information is available, while MMSED minimizes the mean square error (MSE) between the transmitted signal and the equalizer output and thus, partially restores the frequency-nonselective channel. The weight matrix  $\mathbf{W}_0(k)$  is given by

$$\mathbf{W}_0(k) = \begin{cases} \left( \tilde{\mathbf{H}}_0^H(k)\tilde{\mathbf{H}}_0(k) \right)^{-1} \tilde{\mathbf{H}}_0^H(k) & \text{for ZFD} \\ \tilde{\mathbf{H}}_0^H(k) \left( \tilde{\mathbf{H}}_0(k)\tilde{\mathbf{H}}_0^H(k) + \frac{\sigma_I^2 + \sigma_n^2}{P} \mathbf{I}_{N_r} \right)^{-1} & \text{for MMSE} \end{cases}, \tag{7}$$

where  $(\cdot)^H$ ,  $\sigma_I^2$ , and  $\sigma_n^2$  denote the Hermitian transpose, the average received interference power, and the noise power, respectively.  $P$  is the normalized transmit signal power which is same for all users in the case of no TPC, while it is the normalized TPC target  $P_{\text{tpc}}$  in the case of TPC. The CCI power  $\sigma_I^2$  and the noise power  $\sigma_n^2$  are given by

$$\begin{cases} \sigma_I^2 = \frac{1}{2} E \left[ |I_{m(0)}(k)|^2 \right] \\ \sigma_n^2 = \frac{1}{2} E \left[ |\Pi_{m(0)}(k)|^2 \right] \end{cases} \text{ for } m(0) = 0 \sim N_r - 1 \tag{8}$$

which must be estimated, but in this paper, they are assumed to be perfectly known at the receiver.

The detector output signal block  $\{\tilde{S}_{u(0)}(k); k = 0 \sim N_c - 1\}$  of the  $u(0)$ -th user in the  $c = 0$ -th cell is transformed by using an  $N_c$ -point IFFT to the time-domain signal block  $\{\tilde{s}_{u(0)}(t); t = 0 \sim N_c - 1\}$  with

$$\tilde{s}_{u(0)}(t) = \frac{1}{N_c} \sum_{k=0}^{N_c-1} \tilde{S}_{u(0)}(k) \exp\left(j2\pi t \frac{k}{N_c}\right), \tag{9}$$

which is the decision variable associated with the  $t$ -th symbol transmitted from the  $u(0)$ -th user. The symbol decision is done as

$$\hat{s}_{u(0)}(t) = \arg \min_{s_{u(0)} \in D} \left| \tilde{s}_{u(0)}(t) - s_{u(0)}(t) \right|, \tag{10}$$

where  $D$  is the set of candidate symbols.

### 3.3 Transmit Power Control

The received signal power varies according to the distance-dependent path loss, shadowing loss, and fading. The signals transmitted from users close to the cell edge are weak and therefore, the bit error rate (BER) performance may degrade. To remedy this performance degradation, TPC can be used. However, in return, the use of TPC may increase the CCI to

**Table 1** Simulation condition

Transmitter	Data modulation	QPSK	
	Number of users per cell	$U = 1 \sim 6$	
	FFT block size	$N_c = 256$	
	Transmit power control	Type	Slow and fast
		Target $E_b/N_0$	$\infty$
Channel	Path-loss exponent	$\alpha = 3.5$	
	Standard deviation of shadowing loss	$\sigma = 7$ dB	
	Fading	Type	Block Rayleigh fading ( $L = 16$ )
		Power delay profile	Uniform
		Time delays	$\tau_l = lT_s, l = 0 \sim L - 1$
Receiver	Number of receive antennas	$N_r = 4, 6, 8$	
	Signal detection	ZFD and MMSED	
	Channel estimation	Ideal	
Required quality	Required BER	$BER_{req} = 10^{-3}$	
	Allowable outage probability	$Q = 0.1$	

other cells. To which extent the MU SC-MIMO multiplexing combined with FDE and TPC can increase the uplink capacity is a practically important problem.

We consider the slow TPC and fast TPC. Slow TPC keeps the local average received signal power (averaged over the fading statistics) always at the prescribed target value, while fast TPC keeps the instantaneous received signal power always at the prescribed target value. The transmit signal power  $P_{u(c)}$  of the  $u$ -th user in the  $c$ -th cell is given as

$$P_{u(c)} = \begin{cases} \frac{P_{tpc}}{r_{c,u(c)}^{-\alpha} \cdot 10^{-\frac{\eta_{c,u(c)}}{10}}} & \text{for slow TPC} \\ \frac{P_{tpc}}{r_{c,u(c)}^{-\alpha} \cdot 10^{-\frac{\eta_{c,u(c)}}{10}} \cdot \frac{1}{N_c \cdot N_r} \sum_{k=0}^{N_c-1} \sum_{m=0}^{N_r-1} |H_{m(c),u(c)}(k)|^2} & \text{for fast TPC} \end{cases}, \quad (11)$$

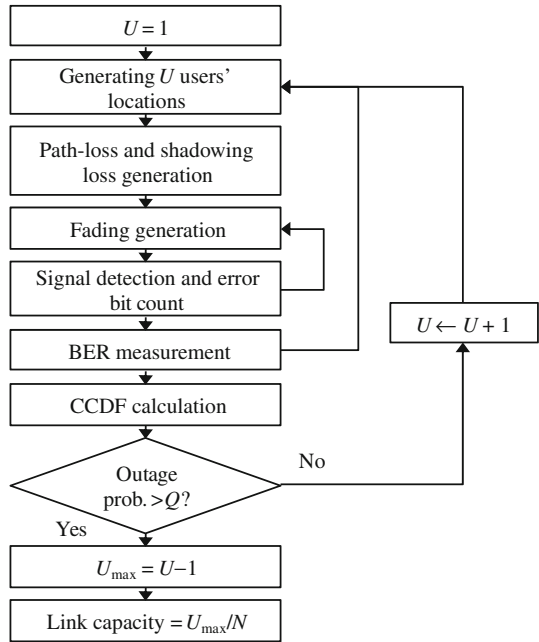
where  $P_{tpc}$ ,  $r_{c,u(c)}^{-\alpha}$ , and  $\eta_{c,u(c)}$  represent the normalized TPC target, the distance-dependent path loss, and the shadowing loss in dB between the  $u$ -th user and its communicating BS of the  $c$ -th cell, respectively.

## 4 Simulation Results

### 4.1 Simulation Procedure

Table 1 summarizes the simulation condition. The channel is assumed to be a frequency-selective block Rayleigh fading having a symbol-spaced  $L = 16$ -path uniform power delay profile, i.e.,  $E \left[ |h_{m(0),u(c)}^{(l)}|^2 \right] = 1/L$  for all  $l$ . It is assumed that the path loss exponent is  $\alpha = 3.5$  and the shadowing loss follows the log-normal distribution with standard deviation  $\sigma = 7$  dB. In this paper, we consider the interference-limited channel condition (i.e.,  $\sigma_n^2 \rightarrow 0$ ).

**Fig. 4** Computer simulation procedure



The computer simulation procedure is illustrated in Fig. 4. First,  $U$  users' locations (starting from  $U = 1$ ) are randomly generated in each cell. The path loss and the shadowing loss are generated for each user. Then,  $L = 16$  path gains associated with each user are generated. The local average BERs for  $U$  users in the  $c = 0$ -th cell are measured. As stated in Sect. 3, we are assuming block fading in which fading stay constant during the transmission of one signal block of  $N_g + N_c$  symbols, but, changes block by block due to the user mobility. In the computer simulation, first we measure the local average BER which is the BER averaged over the fading statistics. The local average BER changes according to the change in user location. The local average BER measurement is repeated a sufficient number of times by changing the user locations to find the complementary cumulative distribution function (CCDF) of the local average BER. The outage probability is the probability of the local average BER exceeding the required BER. If the outage probability is less than the allowable outage probability, the number  $U$  of users is incremented by one. We introduce the normalized uplink capacity defined as the maximum number  $U_{\max}$  of supportable users normalized by the cluster size  $N$ . In this paper, the required BER,  $\text{BER}_{\text{req}}$ , and the allowable outage probability  $Q$  are set as  $\text{BER}_{\text{req}} = 10^{-3}$  and  $Q = 0.1$ , respectively.

As the benchmark comparison, we also evaluate the BER performance achievable using single-user (SU) SC-SIMO diversity (using MMSE-FDE) [24]. The output vector of the SU SC-SIMO diversity combiner, corresponding to Eq. (6), is given as

$$\tilde{S}_{u(0)}(k) = \mathbf{Y}_0^T(k) \cdot \mathbf{w}_{u(0)}(k), \tag{12}$$

where  $\mathbf{w}_{u(0)}(k)$  is the antenna weight vector given as

$$\mathbf{w}_{u(0)}(k) = \frac{\tilde{\mathbf{H}}_{u(0)}^*(k)}{\left\| \tilde{\mathbf{H}}_{u(0)}(k) \right\|^2 + \frac{\sigma_I^2 + \sigma_n^2}{P}} \tag{13}$$



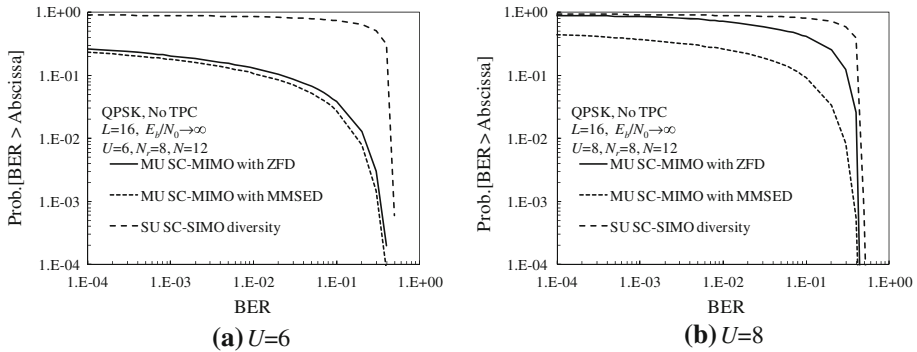


**Fig. 5** CCDFs of local average BER.

with  $\|\cdot\|$  representing the vector norm operation and  $P$  is the same as in Eq. (7). Note again that we are assuming the interference-limited condition,  $\sigma_n^2 \rightarrow 0$  in Eq. (13).

### 4.2 BER Distribution

Figure 5 illustrates the CCDF of the local average BER for the case of  $N_r = 8$  (the number of receive antennas),  $L = 16$  (the number of paths), and  $N = 12$  (the cluster size). No TPC is assumed. ZF has a problem of noise plus CCI enhancement resulting from the restoration of the channel frequency-nonselctivity. However, it can be seen from Fig. 5a that when  $U = 6$  (the number of users), ZFD provides almost the same outage probability as MMSED. The reason for this is explained below. The received SINR in a Rayleigh fading channel is chi-square distributed with the degree of freedom of  $2(N_r - U + 1)$  for both ZFD and MMSED [25, 26] and hence, both ZFD and MMSED achieve the same  $(N_r - U + 1)$ -th diversity order [27]. When  $U$  is smaller than  $N_r$ , diversity order of higher than one is achieved. In this case, ZF can mitigate the CCI enhancement problem and hence, ZF approaches MMSED. On the other hand, when  $U = N_r = 8$  (see Fig. 5b), both ZFD and MMSED have a diversity order of one. In this case, ZF suffers from the CCI enhancement problem and therefore, ZF gives the higher outage probability than MMSED. On the other hand, SU SC-SIMO diversity is the single-user detection and hence, its BER performance significantly degrades due to large intra-cell interference in addition to the CCI from surrounding co-channel cells. This leads to always higher outage probability than those of ZFD and MMSED.

Below, we discuss how much MU SC-MIMO multiplexing can increase the normalized uplink capacity (defined by  $U_{\max}/N$ ) compared to SU SC-SIMO diversity. We also discuss the impacts of the number  $N_r$  of receive antennas and TPC.

### 4.3 Uplink Capacity

Figure 6 plots the normalized uplink capacity as a function of the cluster size  $N$ . No TPC is assumed. SU SC-SIMO diversity can always accommodate single user only ( $U_{\max} = 1$ ). It can be seen from Fig. 6a that when  $N_r = 4$ , the normalized uplink capacity can be maximized at  $N = 12$  for MU SC-MIMO by using either ZFD or MMSED and it is  $U_{\max}/N = 0.166$ . On the other hand, the normalized uplink capacity is maximized at  $N = 4$  for SU SC-SIMO diversity and it is  $U_{\max}/N = 0.143$  which is only slightly lower than MU SC-MIMO. When  $N_r$  is increased to 8 (see Fig. 6b), the normalized uplink capacity is maximized at  $N = 9$  for MU SC-MIMO multiplexing by using either ZFD or MMSED and it is  $U_{\max}/N = 0.333$

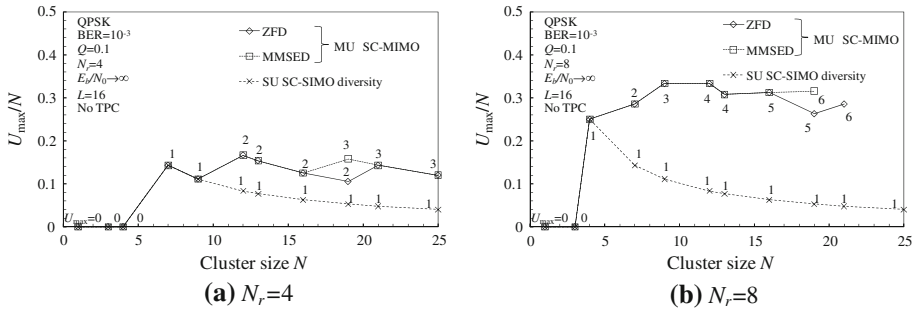


Fig. 6 Normalized uplink capacity

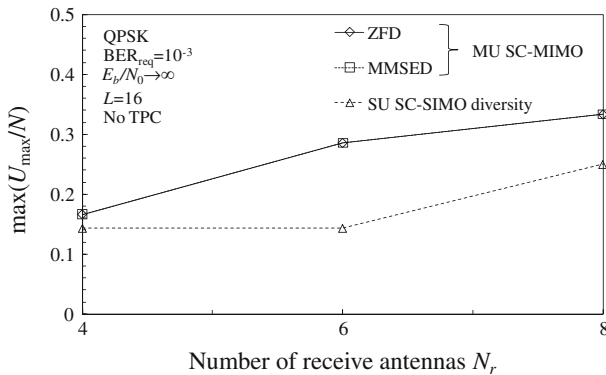


Fig. 7 Impact of  $N_r$

which is about 1.3 times higher than that of SU SC-SIMO diversity (the maximum value of  $U_{\max}/N$  is 0.25 at  $N = 4$ ).

There is a trade-off relationship between the number of users and the diversity order (remember that the diversity order of MU SC-MIMO multiplexing is given by  $N_r - U + 1$ ). When  $U = N_r$ , both ZFD and MMSED have the diversity order of one and therefore, the cluster size  $N$  must be large enough to sufficiently reduce the CCI, leading to the decreased uplink capacity. The maximum normalized uplink capacity is obtained from Fig. 6 which plots  $U_{\max}/N$  curves as a function of  $N$ . Figure 7 illustrates the impact of  $N_r$  (the number of receive antennas) on the normalized uplink capacity of MU SC-MIMO multiplexing. Increasing  $N_r$  is quite effective to increase the uplink capacity; MU SC-MIMO multiplexing can increase the uplink capacity almost two times by increasing  $N_r$  from 4 to 8. ZFD and MMSED can achieve almost the same uplink capacity irrespective of  $N_r$ . This is because, as discussed in Sect. 4.2, both ZFD and MMSED can achieve the same  $N_r - U + 1$ -th diversity order as far as  $U < N_r$ .

#### 4.4 Impact of TPC

Figure 8 compares the effects of slow TPC and fast TPC. Both TPC provide almost the same maximum uplink capacity. This is because the block averaged received signal power is given by  $\frac{1}{N_c \cdot N_r} \sum_{k=0}^{N_c-1} \sum_{m=0}^{N_r-1} |H_{m(c),u(c)}(k)|^2$  and its variation is very shallow in a strong frequency-selective channel (since  $L = 16$ ). This can be understood from Fig. 9 which

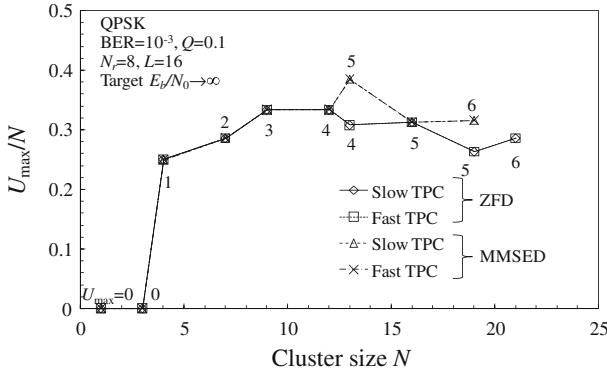


Fig. 8 Comparison of slow TPC and fast TPC

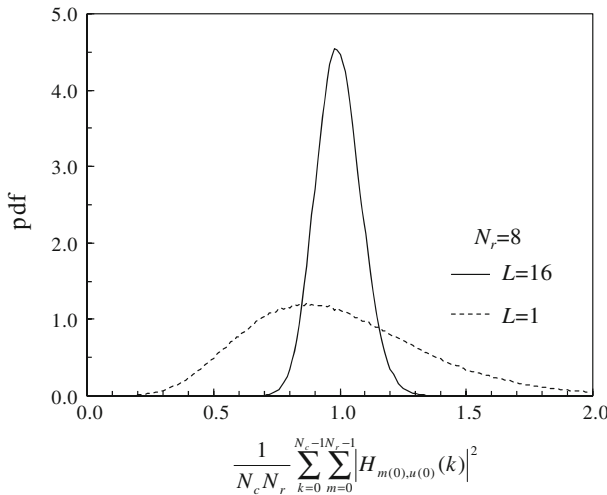


Fig. 9 Pdf of block averaged received signal power

illustrates the probability distribution function (pdf) of the block averaged received signal power. An advantage of fast TPC diminishes and slow TPC can be used.

Figure 10 compares the normalized uplink capacities of MU SC-MIMO multiplexing and SU SC-SIMO diversity both using slow TPC. MU SC-MIMO multiplexing using ZF can achieve almost the same maximum uplink capacity as that using MMSED which is  $U_{max}/N = 0.385$  at  $N = 13$  and is about 1.5 times higher than SU SC-SIMO diversity ( $U_{max}/N = 0.25$  at  $N = 4$ ).

### 5 Conclusions

In this paper, we investigated the uplink capacity of MU SC-MIMO multiplexing combined with FDE and TPC in a broadband cellular system. ZFD and MMSED were considered as the signal detection method. The effects of slow and fast TPC were compared to show that ZFD and MMSED provide almost the same uplink capacity in a strong frequency-selective channel. An advantage of fast TPC diminishes and slow TPC can be used since the block averaged

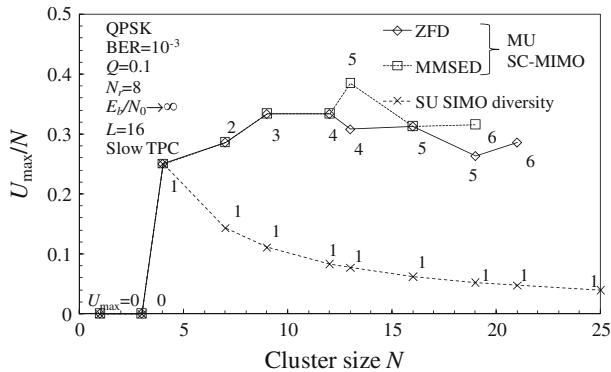


**Fig. 10** Normalized uplink capacity when slow TPC is used

received signal power variation is very shallow in a strong frequency-selective channel. This suggests that in a broadband cellular system, MU SC-MIMO multiplexing using computationally efficient ZFD can be used together with slow TPC. With  $N_r = 8$  and slow TPC, MU SC-MIMO multiplexing using ZFD can achieve about 1.5 times higher uplink capacity than SU SC-SIMO diversity.

In the future broadband wireless systems, the cell size will be reduced to solve the transmit power problem and hence, the propagation channel may become a line of sight (LoS) channel similar to the indoor environment [28]. The investigation of uplink capacity in such a LoS environment is quite important. This is left as an important future study.

## References

- Adachi, F. (2001). Wireless past and future-evolving mobile communications systems. *IEICE Transactions Fundamentals of Electronics*, 84(A1), 55–60.
- Proakis, J. G. (2001). *Digital communications* (4th ed.). New York: McGraw-Hill.
- Falconer, D., Ariyavistakul, S. L., Benyamin-Seeyer, A., & Eidson, B. (2002). Frequency domain equalization for single-carrier broadband wireless systems. *IEEE Communication Magazine*, 40(4), 58–66.
- Adachi, F., Garg, D., Takaoka, S., & Takeda, K. (2005). Broadband CDMA techniques, Special Issue on Modulation, Coding and Signal Processing. *IEEE Wireless Communications Magazine*, 12(2), 8–18.
- Jakes, W. C., Jr. (Ed.). (1974). *Microwave mobile communications*. New York: John Wiley & Sons.
- Gesbert, D., Kountouris, M., Heath, R. W., Jr., Chae, C. B., & Salzer, T. (2007). Shifting the MIMO paradigm: From single user to multiuser communications. *IEEE Signal Processing Magazine*, 24(5), 36–46.
- Spencer, Q. H., Peel, C. B., Swindlehurst, A. L., & Haardt, M. (2004). An introduction to the multi-user MIMO downlink. *IEEE Communications Magazine*, 42(10), 60–67.
- Suard, B., Xu, G., Liu, H., & Kailath, T. (1998). Uplink channel capacity of space-division-multiple-access schemes. *IEEE Transactions Information Theory*, 44(4), 1468–1476.
- Sfar, S., Murch, R. D., & Letaief, K. B. (2003). Layered space-time multiuser detection over wireless uplink systems. *IEEE Transactions Wireless Communications*, 2(4), 653–668.
- Ekstrom, H., Furuskar, A., Karlsson, J., Meyer, M., Parkvall, S., Torsner, J., & Wahlqvist, M. (2006). Technical solutions for the 3G long-term evolution. *IEEE Communications Magazine*, 44(3), 38–45.
- Guo, L., & Huang, Y. (2005). A Multi-user SC-FDE-MIMO system for frequency-selective channels. In *Thirty-Ninth Asilomar conference on signals, systems and computers*, pp. 1593–1597.
- Vandenameele, P., der Perre, L. V., Gyselinckx, B., Engels, M., Moonen, M., & Man, H. D. (2000). A single-carrier frequency-domain SDMA basestation. In *Proceedings IEEE international conference on acoustics, speech, and signal processing*, pp. 3714–3717.
- Coon, J. P., & Beach, M. A. (2002). An investigation of MIMO single-carrier frequency domain MMSE equalization. In: *Proceedings London communications symposium*, pp. 237–240.

14. Rappaport, T. S. (1996). *Wireless communications*. Englewood Cliffs, NJ: Prentice Hall.
15. Dohi, T., Sawahashi, M., & Adachi, F. (1995). Performance of SIR based power control in the presence of non-uniform traffic distribution. In *Fourth IEEE international conference on universal personal communications*, pp. 334–338.
16. Kaltakis, D., Katranaras, E., Imran, M. A., & Tzaras, C. (2009). Information theoretic capacity of Gaussian cellular multiple-access MIMO fading channel. *IET Communications*, 3(7), 1201–1207.
17. Aktas, D., Bacha, M. N., Evans, J. S., & Hanly, S. V. (2006). Scaling results on the sum capacity of cellular networks with MIMO links. *IEEE Transactions on Information Theory*, 52(7), 3264–3274.
18. Chatzinotas, S., Imran, M., & Hoshyar, R. (2009). On the multicell processing capacity of the cellular MIMO uplink channel in correlated rayleigh fading environment. *IEEE Transactions on Wireless Communications*, 8(7), 3704–3715.
19. Jian, L., Kortke, A., & Keusgen, W. (2009). Antenna diversity schemes for uplink frequency-domain multiuser detection in CP-assisted DS-CDMA systems. In *IEEE international conference on communications*, pp. 1–5.
20. El-Sallabi, H., Baum, D. S., Zetterberg, P., Kyosti, P., Rautiainen, T., & Schneider, C. (2006). Wideband spatial channel model for MIMO systems at 5 GHz in indoor and outdoor environments. In *IEEE 63rd vehicular technology conference*, 6, pp. 7–10.
21. Skentos, N. D., Kanatas, A. G., & Constantinou, P. (2006). Multipath parameter results for short range urban propagation environments. In *IEEE international conference on wireless and mobile computing, networking and communications*, pp. 413–418.
22. Huang, H., & Valenzuela, R. A. (2005). Fundamental simulated performance of downlink fixed wireless cellular networks with multiple antennas. In *IEEE 16th international symposium on personal, indoor and mobile radio communications*, pp. 161–165.
23. Huang, H., Trivellato, M., Hottinen, A., Shafi, M., Smith, P., & Valenzuela, R. (2009). Increasing downlink cellular throughput with limited network MIMO coordination. *IEEE Transactions on Wireless Communications*, 8(6), 2983–2989.
24. Adachi, F., & Sao, T. (2003). Joint antenna diversity and frequency-domain equalization for multi-rate MC-CDMA. *IEICE Transactions Communications*, E86-B(11), 3217–3224.
25. Chen, C., & Wang, L. (2005). On the performance of the zero-forcing receiver operating in the multiuser MIMO system with reduced noise enhancement effect. In *Proceedings IEEE global telecommunications conference*, pp. 1294–1298.
26. Gore, D. A., Heath, R. W., & Paulraj, A. J. (2002). Transmit selection in spatial multiplexing systems. *IEEE Communications Letters*, 6(11), 491–493.
27. Winters, J. H., Salz, J., & Gitlin, R. D. (1994). The impact of antenna diversity on the capacity of wireless communication systems. *IEEE Transactions on Communications*, 42(2/3/4), 1740–1751.
28. Bauch, G., Bach Andersen, J., Guthy, C., Herdin, M., Nielsen, J., Nossek, J. A., Tejera, P., & Utschick, W. (2007). Multiuser MIMO channel measurements and performance in a large office environment. In *IEEE wireless communications and networking conference*, pp. 1900–1905.

## Author Biographies



**Takahiro Chiba** received his B.E. and M.E. degrees in communications engineering from Tohoku University, Sendai, Japan, in 2007 and 2009, respectively. He joined NTT Network Innovation Laboratories, Yokosuka, Japan, in 2009, and has been engaged in the research of signal processing.



**Kazuaki Takeda** received his B.E., M.S. and Dr. Eng. degrees in communications engineering from Tohoku University, Sendai, Japan, in 2003, 2004, and 2007, respectively. Since 2005, he was a Japan Society for the Promotion of Science (JSPS) research fellow. In 2008, he joined NTT DOCOMO INC. His research interests include equalization, interference cancellation, transmit/receive diversity and multiple access techniques. He was a recipient of the 2003 IEICE RCS (Radio Communication Systems) Active Research Award and 2004 Inose Scientific Encouragement Prize.



**Kazuki Takeda** received his B.S. and M.S. degrees in communications engineering from Tohoku University, Sendai, Japan, in 2006 and 2008. Currently he is a Japan Society for Promotion of Science (JSPS) research fellow, studying toward his Ph.D. degree at the Department of Electrical and Communications Engineering, Graduate School of Engineering, Tohoku University. His research interests include precoding and channel equalization techniques for mobile communication systems.



**Fumiuyuki Adachi** received the B.S. and Dr. Eng. degrees in electrical engineering from Tohoku University, Sendai, Japan, in 1973 and 1984, respectively. In April 1973, he joined the Electrical Communications Laboratories of Nippon Telegraph & Telephone Corporation (now NTT) and conducted various types of research related to digital cellular mobile communications. From July 1992 to December 1999, he was with NTT Mobile Communications Network, Inc. (now NTT DoCoMo, Inc.), where he led a research group on wide-band/broadband CDMA wireless access for IMT-2000 and beyond. Since January 2000, he has been with Tohoku University, Sendai, Japan, where he is a Professor of Electrical and Communication Engineering at the Graduate School of Engineering. His research interests are in CDMA wireless access techniques, equalization, transmit/receive antenna diversity, MIMO, adaptive transmission, and channel coding, with particular application to broadband wireless communications systems. From October 1984 to September 1985, he was a United Kingdom SERC Visiting Research Fellow in the Department of Electrical

Engineering and Electronics at Liverpool University. He is an IEICE Fellow and was a co-recipient of the IEICE Transactions best paper of the year award 1996 and again 1998 and also a recipient of Achievement award 2003. He is an IEEE Fellow and was a co-recipient of the IEEE Vehicular Technology Transactions best paper of the year award 1980 and again 1990 and also a recipient of Avant Garde award 2000. He was a recipient of Thomson Scientific Research Front Award 2004, Ericsson Telecommunications Award 2008, Telecom System Technology Award 2010, and Prime Minister Invention Prize 2010.